Translational Oncology
www.transonc.com

Volume 13 Number 2 February 2020 pp. 201–211 201

RUNX2/CBFB modulates the response to MEK inhibitors through activation of receptor tyrosine kinases in *KRAS*-mutant colorectal cancer

Tonći Šuštić, Evert Bosdriesz, Sake van Wageningen, Lodewyk F.A. Wessels and René Bernards

Division of Molecular Carcinogenesis, Oncode Institute, The Netherlands Cancer Institute, Plesmanlaan 121, Amsterdam, 1066, CX, the Netherlands

Abstract

Intrinsic and acquired resistances are major hurdles preventing the effective use of MEK inhibitors for treatment of colorectal cancer (CRC). Some 35–45% of colorectal cancers are *KRAS*-mutant and their treatment remains challenging as these cancers are refractory to MEK inhibitor treatment, because of feedback activation of receptor tyrosine kinases (RTKs). We reported previously that loss of *ERN1* sensitizes a subset of *KRAS*-mutant colon cancer cells to MEK inhibition. Here we show that the loss of *RUNX2* or its cofactor *CBFB* can confer MEK inhibitor resistance in CRC cells. Mechanistically, we find that cells with genetically ablated *RUNX2* or *CBFB* activate multiple RTKs, which coincides with high SHP2 phosphatase activity, a phosphatase that relays signals from the cell membrane to downstream pathways governing growth and proliferation. Moreover, we show that high activity of SHP2 is causal to loss of *RUNX2*-induced MEK inhibitor resistance, as a small molecule SHP2 inhibitor reinstates sensitivity to MEK inhibitor in *RUNX2* knockout cells. Our results reveal an unexpected role for loss of *RUNX2/CBFB* in regulating RTK activity in colon cancer, resulting in reduced sensitivity to MEK inhibitors.

Translational Oncology (2020) 13, 201–211

Introduction

KRAS-mutant colorectal cancers (CRCs) are highly refractory to targeted treatments, including inhibition of direct downstream targets of KRAS, such as MEK [1–3]. We reported previously that genetic ablation of the endoplasmatic reticulum–embedded kinase ERN1 sensitizes *KRAS*-mutant colorectal cancer cells to MEK inhibition [4]. To reveal the mechanistic connection between ERN1 and the MAPK signaling pathway, we performed a genome-wide CRISPR/Cas9 genetic screen in *ERN1* knockout (KO) cells to find modulators of the MEK inhibitor response. Using this approach, we identified a number of genes whose inactivation can support the growth and proliferation of *ERN1* KO cells in the presence of MEK inhibitor [4]. Besides previously validated genes, *DUSP4*, *DET1*, and *COP1*, we also identified in the same genetic screen *RUNX2* (formerly known as core-binding factor subunit alpha-1 or *CBFA1*) and its transcriptional coactivator; *CBFB* (core-binding factor subunit beta) as regulators of the MEK inhibitor response [4].

The RUNX (runt-related) family of transcription factors are heterodimeric proteins composed of a DNA-binding alpha subunit and a non-DNA–binding beta subunit. All three mammalian RUNX proteins (RUNX1, RUNX2, and RUNX3) bind to a common DNA motif and heterodimerize with CBFβ, which facilitates DNA binding of RUNX proteins without making a direct contact with DNA itself [5]. The functional and mechanistic interaction between RUNX2/CBFA1 and CBFβ has been well documented using various in vitro [6] and in vivo model systems [7–10]. While all three RUNX proteins are involved in skeletal development and differentiation, RUNX2 is best characterized in terms of its role in control of bone cell proliferation and differentiation [11]. RUNX2 is often referred to as the principal osteogenic master switch, as it is essential for the formation of mature osteocytes and for controlling the expression of genes required for mineralization of the bone extracellular matrix.

Address all correspondence to: René Bernards The Netherlands Cancer Institute, Plesmanlaan 121, 1066, CX, Amsterdam, the Netherlands. E-mail: r.bernards@nki.nl.
Received 4 October 2019; Accepted 10 October 2019

1936-5233/19
https://doi.org/10.1016/j.tranon.2019.10.006

Heterozygous loss of *RUNX2* causes the skeletal disease cleidocranial dysplasia [12], whereas mice with a homozygous mutation in the *Runx2* locus die at birth without breathing, because of complete lack of ossification (bone formation) [13,14]. In normal development, *RUNX2* is robustly expressed during early embryogenesis, before formation of bone tissue, and its functional relevance at later stages of development remains less defined. It is, however, known that RUNX2 can regulate cell migration [15] and vascular invasion in bone tissue [16]. These were the first findings supporting the role of *RUNX2* in cell fate determination in cells that are not of osteogenic lineage.

RUNX2 is regulated by a number of posttranscriptional control mechanisms including selective proteolysis and phosphorylation. Specific ERK/MAPK phosphorylation sites on RUNX2 have been identified and functionally characterized, which suggest that RUNX2 is activated by the MAPK pathway [17,18]. Here, we set out to investigate how the loss of either *RUNX2* or *CBFB* can cause MEK inhibitor resistance in colorectal cancer. Our studies reveal an unexpected role for *RUNX2* in controlling signaling through the MAP kinase pathway through regulation of multiple RTKs.

Materials and Methods

Cell Culture, Transfection, and Lentiviral Infection

We used HEK293 cells, cultured in DMEM, for lentiviral production. All other cell lines were maintained in RPMI1640 medium containing 10% FBS and 1% penicillin/streptomycin at 37 °C and 5% CO_2. All cell lines were purchased from the American Type Culture Collection (ATCC), STR profiled (by Eurofins Medigenomix Forensik GmbH, Ebersberg, Germany) and routinely tested negative for mycoplasma. Transfection of HEK293 cells with linear polyethylenimine (PEI) 25K from polysciences (cat# 23966-2) and subsequent infection of target cells was performed as described previously [19]. For knockout of individual genes, the following single guide (sg) RNAs were cloned in the lenti CRISPR version 2.1 (LC2.1) vector by Gibson cloning: sgERN1, 5′-ACATCCCGAGA-CACGGTGGT-3’; sgRUNX2, 5′-GCTGTCGGTGCGGAC-GAGTT-3’; sgCBFB, 5′-GCCGACTTACGATTTCCGAG-3’. Nontargeting (NT) sgRNA 5′-ACGGAGGCTAAGCGTCGCAA-3′ was used as a control.

Cell Proliferation Assays and Growth Curves

For long-term cell proliferation assays cells were seeded in 6-well plates at densities of around 1×10^4 cells per well, in 12-well plates at around 5×10^3 cells per well, or in 48-well plates at around 2×10^3 cells per well, and cultured with or without inhibitors, as indicated. When control cells reached confluency, all cells were fixed in 4% formaldehyde and stained with 0.1% crystal violet (in water).

For short-term growth inhibition assays, cells were seeded in 96-well plates at around 800 cells per well. Twenty-four hours after seeding, serial dilutions of AZD6244 were added to cells to final drug concentrations ranging from 0.04 to 10 μM. Cells were then incubated for 72 hours and cell viability was measured using the CellTiter-Blue Viability Assay (Roche). Relative survival in the presence of AZD6244 was normalized to the untreated controls after subtracting the background.

Live cell growth was measured by automated determination of confluency every 4 hours using IncuCyte Zoom (Essen Bioscience). Between 600 and 800 cells were plated per well of a 96-well plate and all experiments were carried out in triplicates. MEK inhibitors selumetinib (AZD6244) and trametinib (GSK1120212) were purchased from Selleck chemicals and kept as 10 mM stock solution aliquots in DMSO. SHP2 inhibitor SHP099 was synthesized as described previously [20]. Afatinib and pan-RAF inhibitor LY3009120 were purchased from MedKoo Inc. and neratinib was purchased from Bio-Connect BV. Anti-EGFR monoclonal antibody cetuximab was obtained from the Hospital Pharmacies at The Netherlands Cancer Institute.

Protein Lysate Preparation and Western Blot Analysis

Cells were lysed and western blots were performed as described previously [19]. Primary antibodies against HSP90 (H-114; sc-13119), ERK1 (C16; sc-93), ERK2 (C14; sc-154), p-ERK1/2 (E-4; sc-7383), and SHP2 (SH-PTP2 C-18; sc-280) were purchased from Santa Cruz Biotechnology. Antibodies against EGFR (ab40815), p-EGFR (Y1068; ab5644), and p-SHP2 (Y542; ab62322) were obtained from Abcam. Antibodies against ERN1 (3294), p-ERK1/2 (9101), RUNX2 (12556), CBFB (12902), JUN (9165), RSK1 (8408), p-p90 RSK (Ser380; 9335), and p-RET (3221) were purchased from Cell Signaling. Antibody against p-RSK1 (Thr359/Ser363; 04-419) was obtained from Millipore. Secondary antibodies were obtained from Bio-Rad Laboratories. Human Phospho-Receptor Tyrosine Kinase Array Kit was purchased from R&D and processed according to manufacturer's instructions. All experiments shown, except RTK array analysis, were performed independently at least three times.

Computational Analysis of Drug Response Data

Drug response and (RMA normalized) *RUNX2* expression and mutation data in colorectal cancer cell lines from the GDSC1000 panel were downloaded from www.cancerrxgene.org [21]. IC50 values of the 5 MEK inhibitors in the panel were median centered to make them comparable. T-tests were performed to assess statistical significance of difference in response between groups.

Analysis of RNA-seq Data

Transcriptomic analysis was performed using the R-package limma [22]. Non- or lowly expressed genes (<1 count per million in at least 2 samples) were removed before analysis. Read counts were transformed using the voom function. Multidimensional scaling (MDS) analysis was performed with the plotMDS function. Because of the transcriptional and phenotypic similarity, the *ERN1/CBFB* and *ERN1/RUNX2* DKO lines were treated as biological replicates. Differential gene expression analysis was performed using a linear model with drug-treatment, *CBFB/RUNX2* KO status, and the interaction between drug-treatment and KO status as variables, using the standard limma functions lmFit and eBayes. Raw and processed data from the next-generation RNA sequencing of samples have been deposited to the NCBI Gene Expression Omnibus (GEO) under accession number GSE139169.

Results

We recently performed a genetic screen for MEK inhibitor resistance in *ERN1* null LoVo CRC cells, which identified both *RUNX2* and *CBFB* as potential modifiers of the response to MEK inhibitors [4]. To validate these findings, we asked whether loss of *RUNX2* or *CBFB* indeed confers resistance to MEK inhibitors in these cells. We introduced gRNAs targeting the *RUNX2* or *CBFB* genes in LoVo *ERN1* KO cells. After selection, we tested the growth of *ERN1/*

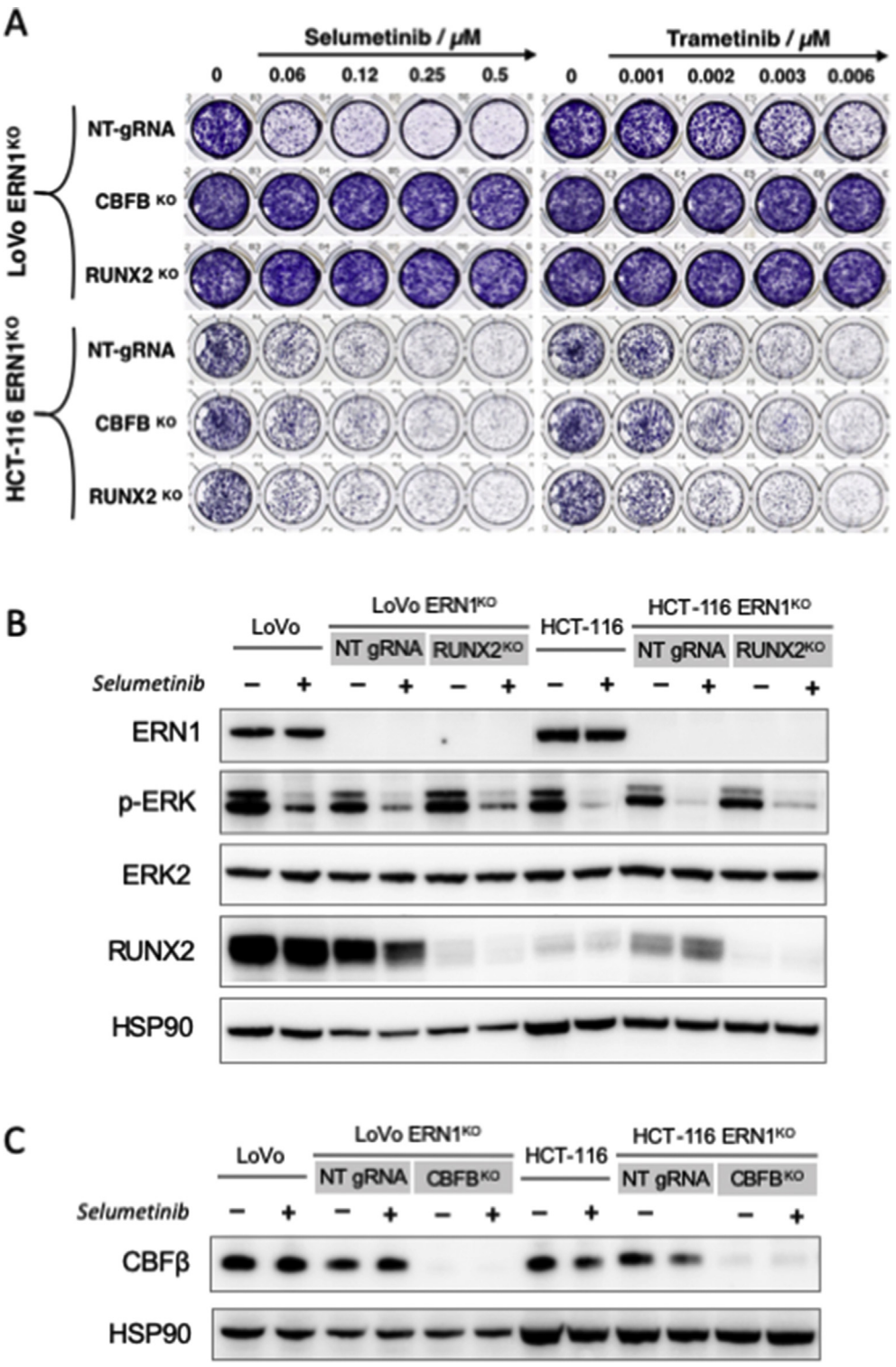

Figure 1. MEK inhibitor sensitivity of LoVo and HCT-116 *ERN1* knockout (KO) cells with loss of *RUNX2* or *CBFB*. (A) Colony formation assays comparing the growth of *CBFB* and *RUNX2* KO cells with cells expressing nontargeting (NT) gRNA in the presence of indicated concentrations of two different MEK inhibitors; selumetinib (left) and trametinib (right). After 10 days of culture, cells were fixed and stained. Image is representative of three independent experiments. (B) Western blot analysis of LoVo and HCT-116 *ERN1/RUNX2* double KO cells compared with parental cells and cells expressing NT gRNA control. All (+) samples were treated with 1 μM of MEK inhibitor selumetinib for 24 hours before collection, and compared with vehicle treated (−) samples. Protein extracts were probed with specific antibodies against ERN1, phosphorylated ERK, ERK2, and RUNX2 (to estimate the efficiency of CRISPR editing in a polyclonal population). Specific antibody against HSP90 was used as a loading control. (C) Western blot analysis of LoVo and HCT-116 *ERN1/CBFB* double KO cells compared with parental cells and cells expressing NT gRNA control. All (+) samples were treated with 1 μM of MEK inhibitor selumetinib for 24 hours before collection, and compared with vehicle treated (−) samples. Protein extracts were probed with specific antibodies against CBFβ (to estimate the efficiency of CRISPR editing), and HSP90 (as a loading control).

RUNX2 double knockout (DKO) and *ERN1/CBFB* DKO cells in the presence and absence of MEK inhibitors selumetinib and trametinib (Figure 1*A*). As predicted by the genetic screen, LoVo *ERN1* KO cells, which are sensitive to low nanomolar amounts of MEK inhibitor, showed strong resistance to MEK inhibitor treatment when gRNAs targeting *RUNX2* or *CBFB* were introduced. We also tested the effect of *RUNX2* or *CBFB* loss in HCT-116 *ERN1* KO cells as an additional model for *ERN1*-loss−induced MEK inhibitor sensitivity. However, we observed no difference in MEK inhibitor response between HCT-116 *ERN1* KO cells transduced with nontargeting (NT) control sgRNA and sgRNAs targeting *RUNX2* or *CBFB* (Figure 1*A*). Biochemical analyses of protein cell lysates showed pronounced levels of RUNX2 protein in LoVo cells, but much lower levels in HCT-116 (Figure 1*B*), which might explain why we observed no change in MEK inhibitor response upon its loss. CBFβ shows similar levels of expression in LoVo and HCT-116 (Figure 1*C*), but its loss also failed to rescue the MEK inhibitor sensitivity of HCT-116 *ERN1* KO cells (Figure 1*A*). This could be explained by the notion that CBFβ acts through RUNX2, which is poorly expressed in HCT-116 cells.

We computationally analyzed *RUNX2* expression in 45 colorectal cancer cell lines from the GDSC1000 panel according to Iorio et al. [21]. Consistent with our Western blot data (Figure 1*B*), we found that HCT-116 cells, unlike LoVo, are on the lower end of the *RUNX2* gene expression scale (Figure 2*A*). Together, these data indicate that expression of *RUNX2* in CRC is rather heterogeneous. Next, we compared the IC50 values of MEK inhibitors of the upper 25% of *RUNX2* expressing cell lines with lower 25% (Supplemental Table 1). The data, represented in a box plot, indicate that *RUNX2* expression levels are not *per se* linked to MEK inhibitor response (Figure 2*B*). However, when we compared cell lines with *RUNX2* mutations to nonmutant cells, we found that *RUNX2* mutant cells have significantly higher MEK inhibitor IC50 values (Figure 2*C*). Considering that *RUNX2* gene does not have a hotspot mutation site, it is likely that the mutations are inactivating. These data suggest that loss of *RUNX2* leads to resistance to MEK inhibitors in CRC. To test directly whether loss of *RUNX2* or *CBFB* could decrease the response of CRC cells to MEK inhibitors in the absence of *ERN1* loss, we made polyclonal populations of *RUNX2* and *CBFB* knockout cells in parental LoVo cells. As can be seen in Figure 2*D*, these polyclonal populations had reduced expression, but not complete loss, of RUNX2 and CBFβ. Nonetheless, this was sufficient to cause a marked increase in resistance to the MEK inhibitor selumetinib (Figure 2*E*). This indicates that *RUNX2* or *CBFB* can modulate MEK inhibitor responses in a broader context than just in cells having *ERN1* loss of function (Figures 2*D* and *E*).

To address the mechanism of loss of *RUNX2*-induced MEK inhibitor resistance, we established a collection of *CBFB* and *RUNX2* KO clones in LoVo in an *ERN1* KO background (Figure 3*A*). For subsequent analyses, we used *CBFB* KO clone B and *RUNX2* KO clone A. We tested the growth properties of these clones in the presence of MEK inhibitor selumetinib using both a colony formation assay (Figure 3*B*) and an IC50 assay (Figure 3*C*). These assays show that the MEK inhibitor resistance induced by the loss of *RUNX2* or *CBFB* surpasses intrinsic resistance of the parental line, as IC50 values of the parental line fall in between values for *ERN1* KO and *ERN1/RUNX2* DKO or *ERN1/CBFB* DKO cells.

To investigate possible transcriptomic changes giving rise to this drug resistance phenotype, we performed RNA sequencing of *CBFB* and *RUNX2* knockout clones (both in the presence and absence of MEK inhibitor). Analysis of RNA sequencing data revealed a strong transcriptional similarity between *CBFB* and *RUNX2* knockout clones indicating a similar resistance mechanism in both clones (Figure 3*D*). Interestingly, *DKK-1* (Dickkopf-1), a secreted inhibitor of the WNT/β-catenin pathway, is the most significant differentially expressed gene when comparing *CBFB* and *RUNX2* knockouts with their parental counterparts (false discovery rate $<10^{-6}$), as shown by a volcano plot in Figure S1*A*. In both treated and untreated conditions, expression levels of *DKK-1* were significantly higher in knockout clones (Figure S1*B*), indicating that RUNX2 might act as a repressor of *DKK-1*.

To further quantify the degree of MEK inhibitor resistance in *CBFB* and *RUNX2* KO cells, we performed IncuCyte® real-time cell proliferation assays using a dose range of the MEK inhibitors selumetinib and trametinib. We compared the response of parental cells to *ERN1* KO cells and confirmed their increased sensitivity to a wide concentration range of the MEK inhibitors selumetinib (Figures 3*E* and *F*) and trametinib (Figures. S2*A* and *B*). On the other hand, *ERN1/RUNX2* DKO cells and *ERN1/CBFB* DKO cells showed uninhibited proliferation in the presence of selumetinib (Figures 3*G* and *H*) or trametinib (Figures S2*C* and *D*) treatment.

In order to delineate the mechanism of *RUNX2*-loss−induced MEK inhibitor resistance, we first analyzed phosphorylation status of a panel of receptor tyrosine kinases using a Human Phospho-Receptor Tyrosine Kinase Array Kit (R&D). The results showed that *ERN1/RUNX2* DKO cells exhibit higher levels of phospho-HER3 (ERBB3) and phospho-RET compared with their parental *ERN1* KO cells, and these differences were even more pronounced under selumetinib treatment (Figure 4*A*). We validated these results by immunoblotting with specific antibodies in both long-term (Figure 4*B*) and short-term assays (Figure 4*C*). Interestingly, prolonged treatment of LoVo cells with MEK inhibitor (14 days) resulted in markedly reduced levels of RUNX2 protein, suggesting that low *RUNX2* expressing cells were positively selected under MEK inhibitor pressure (Figure 4*B*). In addition, we note that *ERN1/RUNX2* DKO cells exhibit sustained levels of phospho-ERK and phospho-RSK despite MEK inhibitor treatment, explaining their poor response to these drugs. Interestingly, this is correlated with high phospho-EGFR as compared with parental LoVo and *ERN1* KO cells. To further confirm the intensity of RTK signaling in *RUNX2* and *CBFB* KO cells, we blotted for phospho-SHP2 (encoded by the *PTPN11* gene), which is essential in signal transduction from the receptor tyrosine kinases in the cell membrane to the RAS-MEK-ERK pathway [23]. Our results show persistent SHP2 activity in *RUNX2* and *CBFB* KO cells compared with MEK inhibitor sensitive *ERN1* KO counterparts. On the other hand, parental LoVo cells exhibit intermediate levels of phospho-SHP2 (Figure 4*C*).

In order to find out whether SHP2 activity is causally related to MEK inhibitor resistance observed in *RUNX2* negative cells, we used SHP2 inhibitor SHP099 and combined it with MEK inhibitor selumetinib in LoVo *ERN1* KO (Figure 5*A*) and *ERN1/RUNX2* DKO cells (Figure 5*B*). As expected, LoVo *ERN1* KO cells were not growing even in relatively modest amounts of selumetinib. However, *ERN1/RUNX2* DKO cells, whose growth was uninhibited in MEK inhibitor alone, exhibited complete growth arrest when SHP2 inhibitor was combined with the MEK inhibitor (Figure 5*B*). Considering that we observed high activity of ERBB3/HER3 in *ERN1/RUNX2* DKO cells (Figure 4*A*), and that ERBB3 is a kinase

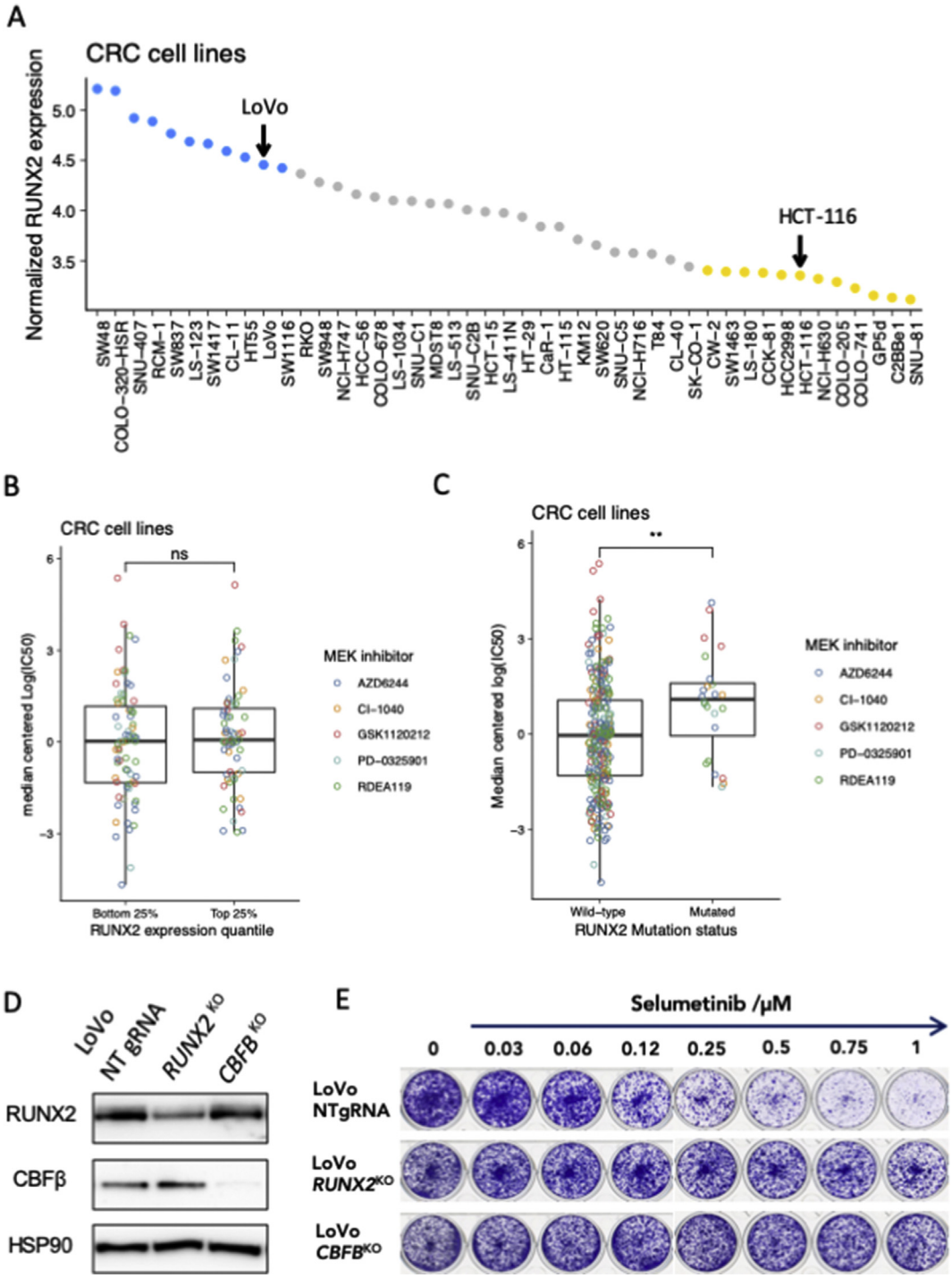

Figure 2. Analyses of RUNX2 expression and mutation status in a CRC panel. MEK inhibitor response of LoVo parental cells with loss of *RUNX2* or *CBFB*. (A) *RUNX2* expression in colorectal cancer cell lines from the GDSC1000 panel. Blue dots represent cell lines in upper-most quantile and yellow dots lowest quantile of *RUNX2* expression. (B) IC50 values for five different MEK inhibitors in lowest 25% *RUNX2* expressing cells (C2BBe1, CCK-81, COLO-205, COLO-741, CW-2, GP5d, HCC-2998, HCT-116, LS-180, NCI-H630, SNU-81 and SW-1463; shown on the left) and highest 25% *RUNX2* expressing cells (CL-11, COLO-320-HSR, HT-55, LS-123, LoVo, RCM-1, SNU-407, SW-1116, SW-1417, SW-48 and SW-837; shown on the right). (C) IC50 values for five different MEK inhibitors in four *RUNX2* mutant CRC cell lines (GP5d, HT-115, SW-620, SW-948; right) compared with nonmutant lines (41 *RUNX2* wild-type CRC cell lines; left). (D) Western blot of LoVo *RUNX2* KO and *CBFB* KO cells compared with NT gRNA controls. (E) Colony formation assay of LoVo *RUNX2* KO and *CBFB* KO cells in the presence and absence of the MEK inhibitor selumetinib, relative to LoVo parental cells expressing nontargeting (NT) gRNA control. Shown is a representative example of three biological replicates.

impaired protein that signals through obligatory heterodimers with other members of the ERBB receptor family, we used EGFR and HER2 inhibitors to see if those could recapitulate the effects of SHP2 inhibition. Interestingly, however, we could not identify a single RTK inhibitor that could mimic the phenotype observed with SHP2 inhibition (Figures S3 *A*–*C*). Only combination of MEK inhibitor

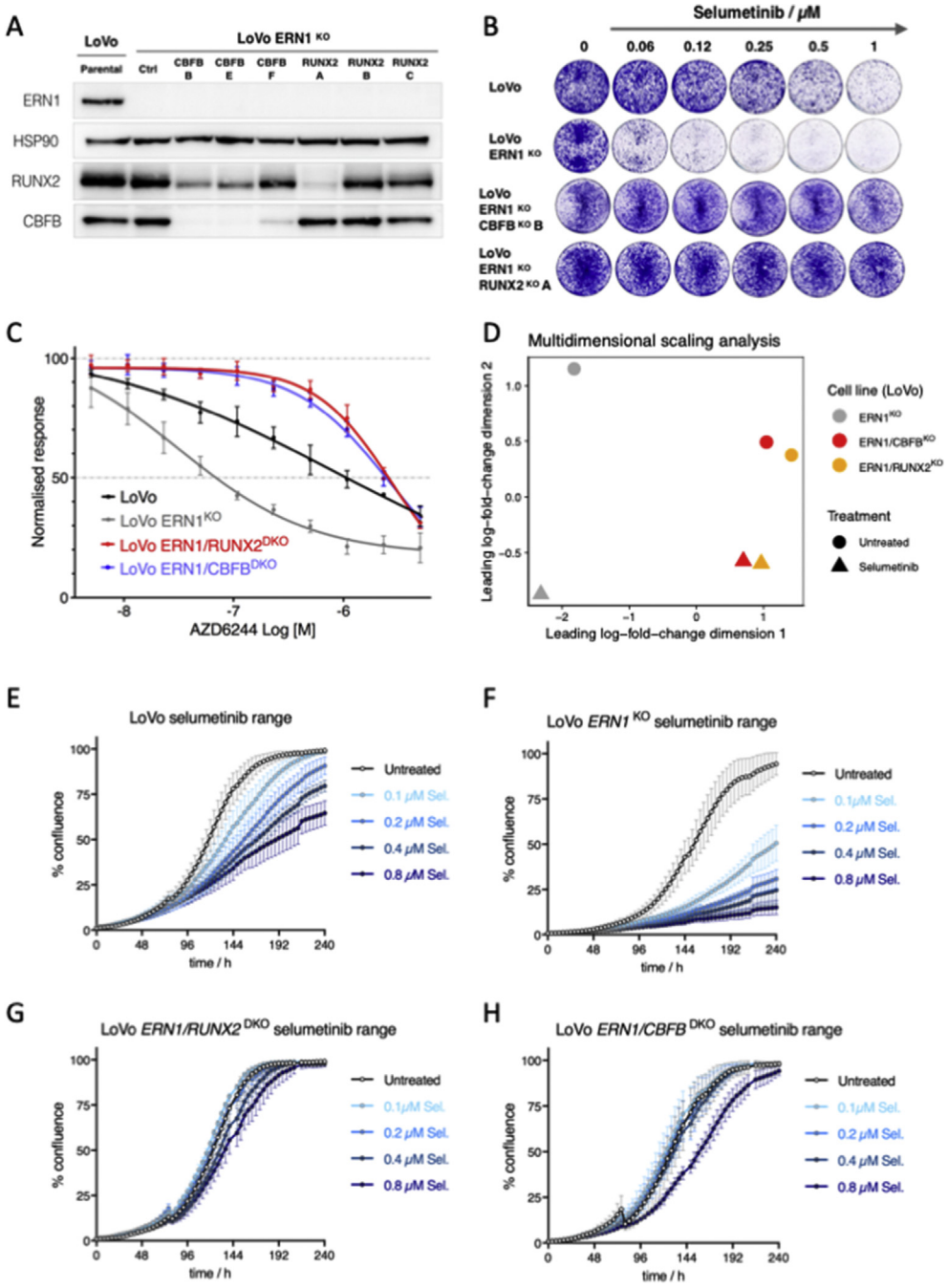

Figure 3. Characterization of LoVo *ERN1/RUNX2* and *ERN1/CBFB* double KO clones. (A) Western blot analysis of LoVo *ERN1/RUNX2* and *ERN1/CBFB* double KO clones. (B) Colony formation assay of *ERN1/RUNX2* and *ERN1/CBFB* double KO cells in the presence and absence of the MEK inhibitor selumetinib, relative to control *ERN1* KO cells and LoVo parental cells. Shown is a representative example of three biological replicates. (C) IC50 growth curves of LoVo *ERN1/RUNX2* and *ERN1/CBFB* double KO cells as compared with LoVo *ERN1* KO and LoVo parental cells in the presence of indicated concentrations of AZD6244 (selumetinib). Error bars represent standard deviation of three independent experiments. (D) Multidimensional scaling (MDS) plot of RNA sequencing data from *ERN1* KO, *ERN1/CBFB* KO and *ERN1/RUNX2* KO cells treated with 1 μM MEK inhibitor selumetinib or vehicle control. (E–H) Live cell proliferation assays of (E) LoVo parental, (F) LoVo *ERN1* KO, (G) LoVo *ERN1/RUNX2* double KO, and (H) LoVo *ERN1/CBFB* double KO cells in the presence and absence of indicated concentrations of MEK inhibitor AZD6244 (selumetinib). Error bars show standard deviation of three experiments.

with pan-RAF inhibitor could replicate synthetic lethality observed with SHP2 and MEK inhibitor combination (Figure 5*C*). To quantify these effects in time-dependent fashion, we used IncuCyte® real time cell proliferation imaging and quantified cell confluence for LoVo *ERN1/RUNX2* DKO cells in the presence and absence of MEK inhibitor selumetinib, SHP2 inhibitor, or their combination. These data again indicated that the combination of a SHP2 and a MEK inhibitor is highly effective in the context of *RUNX2* null colorectal cancer cells (Figure 5*D*), highlighting the central role of RTK signaling in the resistance to MEK inhibitors of *RUNX2* KO cells.

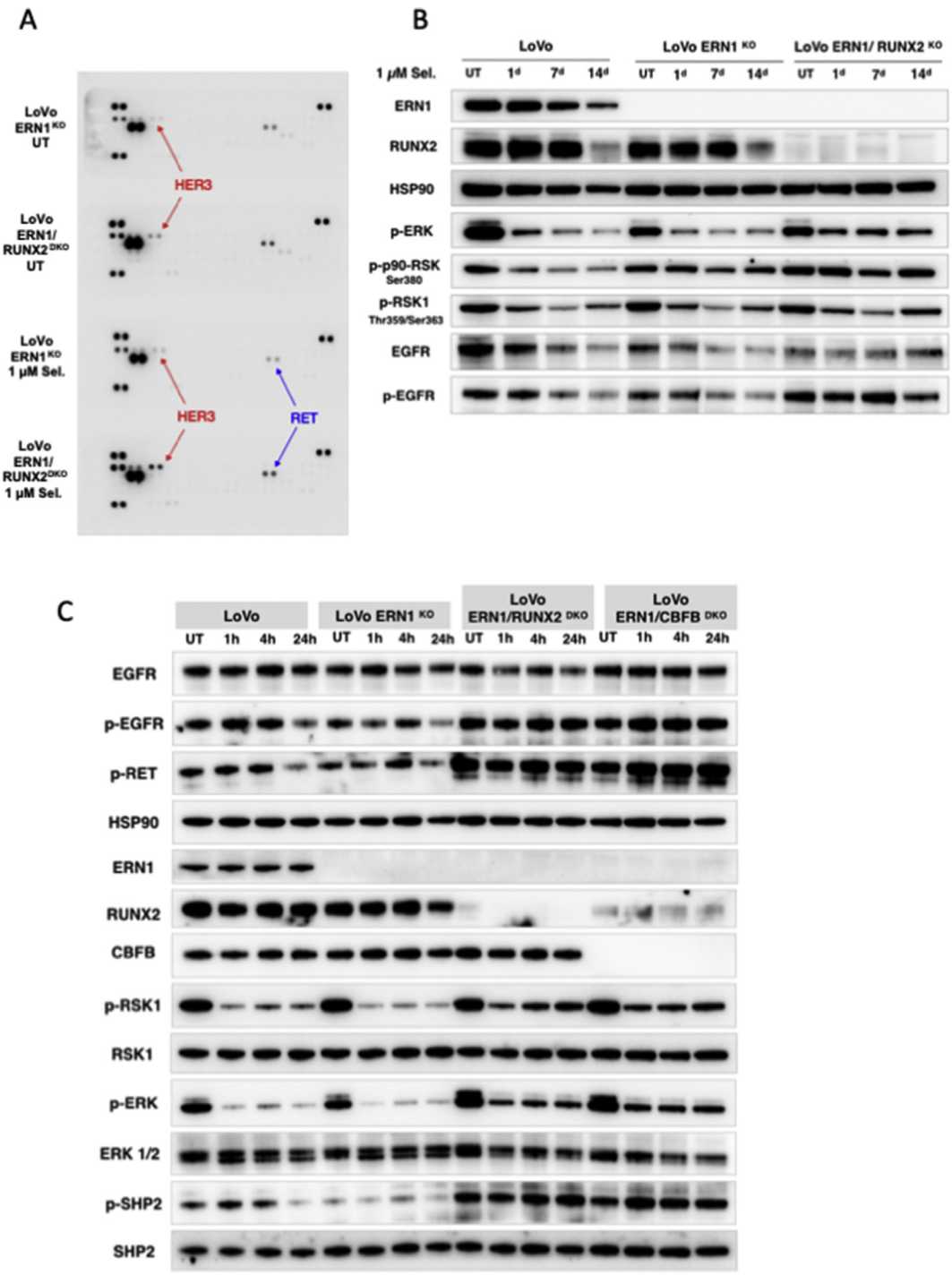

Figure 4. Loss of *RUNX2* induces multiple receptor tyrosine kinases (RTKs). (A) LoVo *ERN1* KO and *ERN1/RUNX2* KO cells were cultured in the presence or absence (untreated = UT) of 1 μM MEK inhibitor selumetinib (1 μM Sel.). After 24 hours, cells were collected and protein lysates were processed with Human Phospho-Receptor Tyrosine Kinase (RTK) Array Kit (R&D) according to manufacturer's instructions. (B) Western blot showing the effects of long-term MEK inhibitor treatment on LoVo, *ERN1* KO and *ERN1/RUNX2* double KO cells. Cells were cultured in the presence and absence of 1 μM selumetinib for the indicated time (in days). (C) Western blot showing the effects of short-term treatment with MEK inhibitor on LoVo parental and LoVo *ERN1* KO cells compared with LoVo *ERN1/RUNX2* and *ERN1/CBFB* double KO cells. Cells were cultured in the presence and absence of 1 μM selumetinib for the indicated time (in hours). All experiments shown, except RTK array analysis, were performed independently at least twice.

Discussion

This study reveals that RUNX2, a critical transcription factor for bone development, and its cofactor CBFβ can regulate MEK inhibitor response in colorectal cancer cells. Previous work has shown that *RUNX2* is aberrantly expressed in cancer cells as compared with normal mammary epithelial cells [24]. In cancer cells, RUNX2 has thus far been shown to regulate beta-casein [25], osteopontin [26], sialoprotein [27], calcitonin, and RANKL [28].

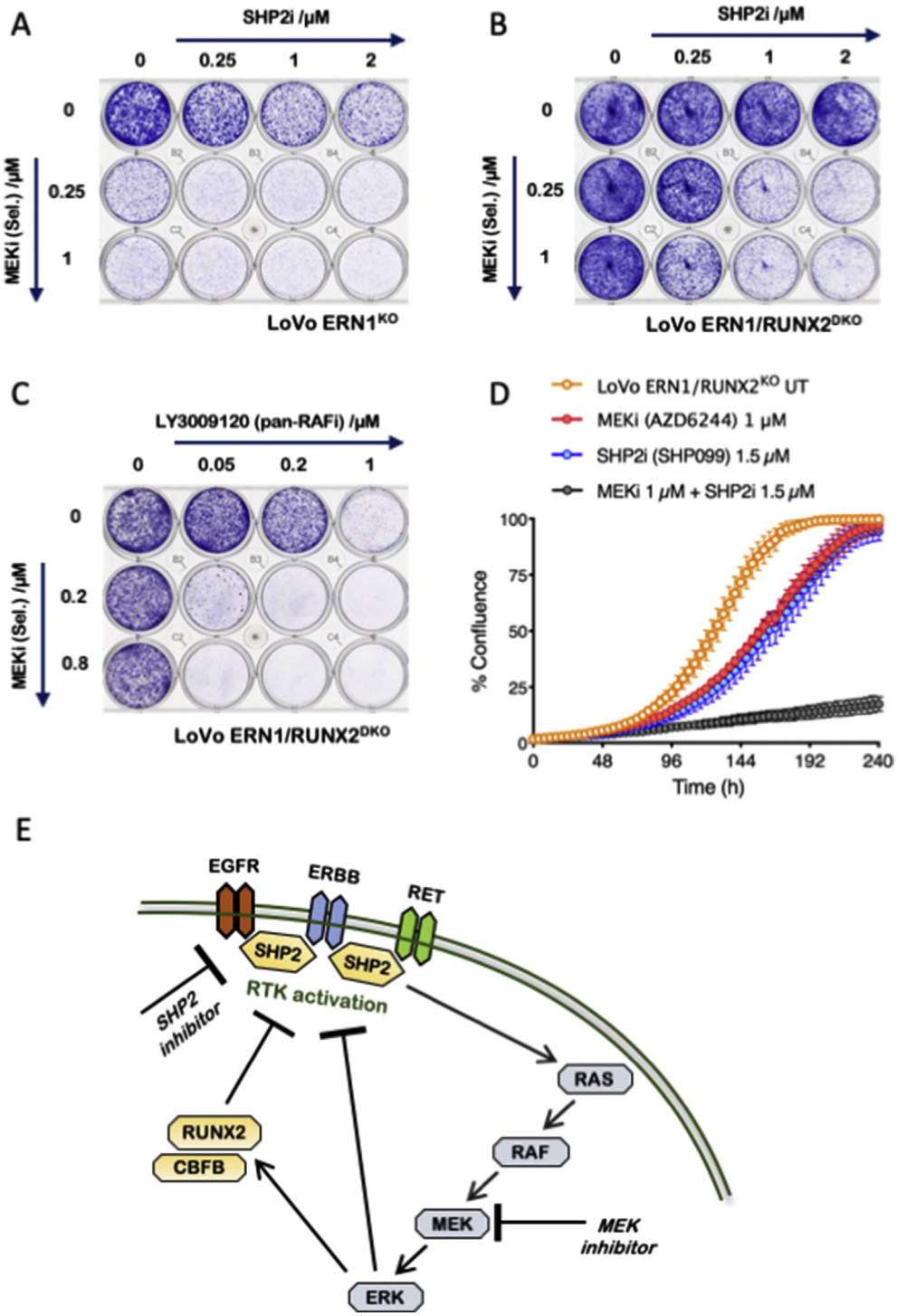

Figure 5. SHP2 is an essential driver of loss of *RUNX2*-induced MEK inhibitor sensitivity. (A) Colony formation assay of LoVo *ERN1* KO cells in the presence of indicated concentrations of the SHP2 inhibitor SHP099 and MEK inhibitor selumetinib. (B–C) Colony formation assays of LoVo *ERN1/RUNX2* double knockout (DKO) cells in the presence and absence of the MEK inhibitor selumetinib (shown vertically) and in the indicated concentrations of (B) SHP2 inhibitor SHP099, and (C) pan-RAF inhibitor LY3009120. Shown are representative examples of three biological replicates. (D) Live cell proliferation assay comparing the growth of LoVo *ERN1/RUNX2* double KO cells in the presence and absence of indicated concentrations of MEK inhibitor selumetinib (AZD6244), SHP2 inhibitor SHP099 and their combination (UT = untreated). Error bars show standard deviation of three experiments. (D) Model showing the interplay between RTK activation, SHP2, RUNX2 and RAS/RAF/MEK/ERK signaling pathway.

More recently, RUNX2 was shown to be required for the growth of multiple myeloma, a malignancy driven by the accumulation and proliferation of abnormal plasma cells in the bone marrow. The suppression of *RUNX2* inhibited the progression of the disease and the expression of metastasis-promoting RUNX2 target genes *RANKL* and *DKK-1* [29]. However, the role of RUNX2 in

regulating the expression or activation of receptor tyrosine kinases or MEK inhibitor sensitivity, in the context of colorectal cancer, has thus far not been identified. In melanoma, however, *RUNX2* knockdown by short hairpin RNAs resulted in RTK downregulation [30]. The same study demonstrated that melanoma cells resistant to the BRAF V600E inhibitor PLX4720 had a significant increase in *RUNX2* expression which was associated with an increase in both RTK expression and activation. This is the opposite of the RUNX2 effect on RTK activity, we find in *KRAS*-mutant colorectal cancer cells. A differential response between melanoma cells and colon cancer cells in terms of their response to inhibition of the MAPK pathway has been shown before by our lab and others [31–33]. In colorectal cancer, unlike melanoma, BRAF inhibition causes rapid feedback activation through the epidermal growth factor receptor (EGFR). For this reason, BRAF inhibitor treatment is ineffective as a monotherapy in colorectal cancer and combination treatment approach is needed. A combination of BRAF inhibitor encorafenib, MEK inhibitor binimetinib, and an EGFR inhibitor cetuximab recently resulted in a successfully completed phase 3 clinical trial [34], underscoring the importance of the regulation of RTK activity in colorectal cancer.

A study by Kim et al. [35] has shown that deletion of *Mek1* and *Mek2* kinases resulted in severe osteopenia and cleidocranial dysplasia, similar to that seen in humans and mice with impaired RUNX2 function. In the present study, we show that RUNX2 directly controls MAPK pathway activity. We first show that loss of RUNX2 reverts the MEK inhibitor sensitivity phenotype of LoVo *ERN1* KO cells. Moreover, lack of *RUNX2* expression increased resistance of parental LoVo cells as well, and this was also confirmed for its binding factor CBFβ. Interestingly, all *CBFB* knockout clones display reduced levels of RUNX2 protein confirming previous findings that CBFβ plays an important role in the stabilization of RUNX proteins by inhibiting ubiquitination-mediated degradation [8,9]. This could explain why whole exome sequencing efforts identified *CBFB* as one of six most significantly mutated genes in breast cancer, right after *TP53*, *PIK3CA,* and *AKT1* [36]. More studies are required to investigate whether *CBFB* loss of function mutations in breast cancer are also associated with increased RTK activity.

Differential gene expression analysis of RNA sequencing data point to genes whose expression pattern changes under MEK inhibitor treatment. Interestingly, transcriptional analysis of *CBFB* and *RUNX2* knockout clones (in the presence and absence of MEK inhibitor) revealed *DKK-1* (Dickkopf-1), a secreted inhibitor of the WNT/β-catenin pathway and a negative regulator of bone formation, as the most significant differentially expressed gene when comparing *CBFB* and *RUNX2* knockouts with their parental counterparts. In both treated and untreated conditions, expression levels of *DKK-1* are significantly higher in knockout clones, indicating that RUNX2 might act as a repressor of *DKK-1*. By contrast, Gowda et al. [29] found that reduced expression of *RUNX2* correlates with a reduction in *DKK-1* in multiple myeloma. Our results suggest context specificity of *DKK-1* regulation by RUNX2. This is potentially significant as it impacts our understanding of WNT signaling regulation in colorectal cancer. For example, Tentler et al. [37] have shown that *DKK-1* is among the core genes in the WNT pathway with increased expression in *KRAS* mutant CRC cells resistant to AZD6244 (selumetinib).

In this work, we demonstrate that RUNX2 functions as a repressor of RTK activity in LoVo colorectal cancer cells. We observed sustained levels of MEK/ERK signaling in *CBFB* or *RUNX2* null cells, even in the presence of MEK inhibitor. These sustained levels of phospho-ERK (resulting in continued proliferation) coincide with high phosphorylation status of EGFR, ERBB3, and RET in *RUNX2* null cells. These findings complement our previous work showing that high RTK activity confers resistance to MEK inhibitors in colon cancer cells [38]. Moreover, here we report high levels of phosho-SHP2 in MEK inhibitor—treated *RUNX2* null cells indicating persistent signaling from the cell membrane which helps to explain the observed resistance phenotype.

To validate the functional significance of SHP2 activity in *RUNX2* negative cells, we used SHP2 inhibitor in combination with MEK inhibitor. The observed synthetic lethality demonstrated that RTK activation in *RUNX2* negative cells is causal to their lack of sensitivity to MEK inhibition. The MEK and SHP2 inhibitor combination has already been demonstrated as a powerful treatment strategy to overcome RTK activity-driven MEK inhibitor resistance; in the context of pancreatic ductal adenocarcinoma [39], *KRAS*-mutant non-small-cell lung cancer [40] and in wild-type *KRAS*-amplified gastroesophageal cancer [41]. In these cancers, combination of SHP2 and MEK inhibitors was shown to synergistically inhibit signaling through the MAPK pathway.

Results presented here suggest that resistance to MEK inhibition via loss or downregulation of *RUNX2* can be circumvented by concomitant treatment with SHP2 inhibitor. This is particularly relevant when we consider that deep deletions of *CBFB* are seen in around 6% of malignant peripheral nerve sheath tumors and in 5% of metastatic prostate cancers (cbioportal.org). Moreover, mutations in *RUNX2* are seen in ~10% of small-cell lung cancer and in ~10% of desmoplastic melanomas [42]. Our data reveal an unexpected relationship between loss of function mutations in *RUNX2* and *CBFB* and activity of RTKs in colon cancer. These data may help explain why loss-of-function mutations in these two genes are seen in a variety of cancers.

Based on our findings and those in the literature, we propose a model for MAPK pathway regulation by RUNX2 (Figure 5*E*). Previous work has shown that RUNX2 expression and activity are positively regulated by the PI3K and MAPK pathways [17,18,43]. Moreover, RUNX2 has been shown to repress RTK signaling [44]. Our present data add to this by showing that the RUNX2/CBFB complex acts as a repressor of RTK activity. Thus, inhibition of MEK has a dual effect on RTK activity. First, ERK inhibition leads to activation of RTK signaling, as previously demonstrated [35,42]. Second, ERK inhibition, by inhibition RUNX2/CBFB activity, also leads to RTK activation (Figure 4). These two effects both counteract the effect of the MEK inhibitor, contributing to drug resistance. In summary, our data are compatible with a model in which *RUNX2* mutant tumors are resistant to MEK inhibitors, but respond to the combination of MEK and SHP2 inhibitors.

Conflict of Interest

The authors declare no conflict of interest.

Credit Author Statement

Tonći Šuštić; : Conceptualization, Investigation, Methodology, Validation, Writing — original draft preparation. Evert Bosdriesz: Formal Analysis, Software, Validation, Data curation, Visualization. Sake van Wageningen: Methodology, Validation. Lodewyk F.A.

Wessels: Supervision, René Bernards: Conceptualization, Writing – Reviewing and Editing, Supervision, Funding Acquisition.

Acknowledgments

The authors thank Cor Lieftink for quality control analysis of the RNA sequencing data and all members of the Bernards, Beijersbergen, van der Heijden, and Wessels groups; in particular Sander Palit and Roderick Beijersbergen for helpful support and discussions. This work was supported by a grant from the Dutch Cancer Society through the Oncode Institute.

Appendix A. Supplementary data

Supplementary data to this article can be found online at https://doi.org/10.1016/j.tranon.2019.10.006.

References

[1] Adjei AA, Cohen RB, Franklin W, Morris C, Wilson D and Molina JR, et al (2008). Phase I pharmacokinetic and pharmacodynamic study of the oral, small-molecule mitogen-activated protein kinase kinase 1/2 inhibitor AZD6244 (ARRY-142886) in patients with advanced cancers. *J Clin Oncol* **26**, 2139–2146. https://doi.org/10.1200/JCO.2007.14.4956.

[2] Migliardi G, Sassi F, Torti D, Galimi F, Zanella ER and Buscarino M, et al (2012). Inhibition of MEK and PI3K/mTOR suppresses tumor growth but does not cause tumor regression in patient-derived xenografts of RAS-mutant colorectal carcinomas. *Clin Cancer Res* **18**, 2515–2525. https://doi.org/10.1158/1078-0432.CCR-11-2683.

[3] Jänne PA, Shaw AT, Pereira JR, Jeannin G, Vansteenkiste J and Barrios C, et al (2013). Selumetinib plus docetaxel for KRAS-mutant advanced non-small-cell lung cancer: a randomised, multicentre, placebo-controlled, phase 2 study. *Lancet Oncol* **14**, 38–47. https://doi.org/10.1016/S1470-2045(12)70489-8.

[4] Sustic T, van Wageningen S, Bosdriesz E, Reid RJD, Dittmar J and Lieftink C, et al (2018). A role for the unfolded protein response stress sensor ERN1 in regulating the response to MEK inhibitors in KRAS mutant colon cancers. *Genome Med* **10**, 90. https://doi.org/10.1186/s13073-018-0600-z.

[5] Cohen MM (2009). Perspectives on RUNX genes: an update. *Am J Med Genet A* **149A**, 2629–2646. https://doi.org/10.1002/ajmg.a.33021.

[6] Mendoza-Villanueva D, Deng W, Lopez-Camacho C and Shore P (2010). The Runx transcriptional co-activator, CBFβ, is essential for invasion of breast cancer cells. *Mol Cancer* **9**, 171. https://doi.org/10.1186/1476-4598-9-171.

[7] Kundu M, Javed A, Jeon J-P, Horner A, Shum L and Eckhaus M, et al (2002). Cbfβ interacts with Runx2 and has a critical role in bone development. *Nat Genet* **32**, 639–644. https://doi.org/10.1038/ng1050.

[8] Lim K-E, Park N-R, Che X, Han M-S, Jeong J-H and Kim S-Y, et al (2015). Core binding factor β of osteoblasts maintains cortical bone mass via stabilization of Runx2 in mice. *J Bone Miner Res* **30**, 715–722. https://doi.org/10.1002/jbmr.2397.

[9] Qin X, Jiang Q, Matsuo Y, Kawane T, Komori H and Moriishi T, et al (2015). Cbfb regulates bone development by stabilizing Runx family proteins. *J Bone Miner Res* **30**, 706–714. https://doi.org/10.1002/jbmr.2379.

[10] Komori T (2003). Requisite roles of Runx2 and Cbfb in skeletal development. *J Bone Miner Res* **21**, 193–197.

[11] Stein GS, Lian JB, van Wijnen AJ, Stein JL, Montecino M and Javed A, et al (2004). Runx2 control of organization, assembly and activity of the regulatory machinery for skeletal gene expression. *Oncogene* **23**, 4315–4329. https://doi.org/10.1038/sj.onc.1207676.

[12] Mundlos S, Otto F, Mundlos C, Mulliken JB, Aylsworth AS and Albright S, et al (1997). Mutations involving the transcription factor CBFA1 cause cleidocranial dysplasia. *Cell* **89**, 773–779.

[13] Komori T, Yagi H, Nomura S, Yamaguchi A, Sasaki K and Deguchi K, et al (1997). Targeted disruption of Cbfa1 results in a complete lack of bone formation owing to maturational arrest of osteoblasts. *Cell* **89**, 755–764.

[14] Otto F, Thornell AP, Crompton T, Denzel A, Gilmour KC and Rosewell IR, et al (1997). Cbfa1, a candidate gene for cleidocranial dysplasia syndrome, is essential for osteoblast differentiation and bone development. *Cell* **89**, 765–771.

[15] Sun L, Vitolo M and Passaniti A (2001). Runt-related gene 2 in endothelial cells: inducible expression and specific regulation of cell migration and invasion. *Cancer Res* **61**, 4994–5001.

[16] Zelzer E, Glotzer DJ, Hartmann C, Thomas D, Fukai N and Soker S, et al (2001). Tissue specific regulation of VEGF expression during bone development requires Cbfa1/Runx2. *Mech Dev* **106**, 97–106.

[17] Xiao G, Jiang D, Thomas P, Benson MD, Guan K and Karsenty G, et al (2000). MAPK pathways activate and phosphorylate the osteoblast-specific transcription factor, Cbfa1. *J Biol Chem* **275**, 4453–4459. https://doi.org/10.1074/jbc.275.6.4453.

[18] Ge C, Xiao G, Jiang D, Yang Q, Hatch NE and Roca H, et al (2009). Identification and functional characterization of ERK/MAPK phosphorylation sites in the Runx2 transcription factor. *J Biol Chem* **284**, 32533–32543. https://doi.org/10.1074/jbc.M109.040980.

[19] Brunen D, de Vries RC, Lieftink C, Beijersbergen RL and Bernards R (2018). PIM kinases are a potential prognostic biomarker and therapeutic target in neuroblastoma. *Mol Cancer Ther* **17**, 849–857. https://doi.org/10.1158/1535-7163.MCT-17-0868.

[20] Garcia Fortanet J, Chen CH-T, Chen Y-NP, Chen Z, Deng Z and Firestone B, et al (2016). Allosteric inhibition of SHP2: identification of a potent, selective, and orally efficacious phosphatase inhibitor. *J Med Chem* **59**, 7773–7782. https://doi.org/10.1021/acs.jmedchem.6b00680.

[21] Iorio F, Knijnenburg TA, Vis DJ, Bignell GR, Menden MP and Schubert M, et al (2016). A landscape of pharmacogenomic interactions in cancer. *Cell* **166**, 740–754. https://doi.org/10.1016/j.cell.2016.06.017.

[22] Ritchie ME, Phipson B, Wu D, Hu Y, Law CW and Shi W, et al (2015). Limma powers differential expression analyses for RNA-sequencing and microarray studies. *Nucleic Acids Res* **43**. https://doi.org/10.1093/nar/gkv007.e47–e47.

[23] Prahallad A, Heynen GJJE, Germano G, Willems SM, Evers B and Vecchione L, et al (2015). PTPN11 is a central node in intrinsic and acquired resistance to targeted cancer drugs. *Cell Rep* **12**, 1978–1985. https://doi.org/10.1016/j.celrep.2015.08.037.

[24] Tandon M, Chen Z and Pratap J (2014). Runx2 activates PI3K/Akt signaling via mTORC2 regulation in invasive breast cancer cells. *Breast Cancer Res* **16**, R16. https://doi.org/10.1186/bcr3611.

[25] Inman CK, Li N and Shore P (2005). Oct-1 counteracts autoinhibition of Runx2 DNA binding to form a novel Runx2/Oct-1 complex on the promoter of the mammary gland-specific gene beta-casein. *Mol Cell Biol* **25**, 3182–3193. https://doi.org/10.1128/MCB.25.8.3182-3193.2005.

[26] Inman CK and Shore P (2003). The osteoblast transcription factor Runx2 is expressed in mammary epithelial cells and mediates osteopontin expression. *J Biol Chem* **278**, 48684–48689. https://doi.org/10.1074/jbc.M308001200.

[27] Barnes GL, Javed A, Waller SM, Kamal MH, Hebert KE and Hassan MQ, et al (2003). Osteoblast-related transcription factors Runx2 (Cbfa1/AML3) and MSX2 mediate the expression of bone sialoprotein in human metastatic breast cancer cells. *Cancer Res* **63**, 2631–2637.

[28] Martin TJ and Gillespie MT (2001). Receptor activator of nuclear factor kappa B ligand (RANKL): another link between breast and bone. *Trends Endocrinol Metab* **12**, 2–4.

[29] Gowda PS, Wildman BJ, Trotter TN, Xu X, Hao X and Hassan MQ, et al (2018). Runx2 suppression by miR-342 and miR-363 inhibits multiple myeloma progression. *Mol Cancer Res* **16**, 1138–1148. https://doi.org/10.1158/1541-7786.MCR-17-0606.

[30] Boregowda RK, Medina DJ, Markert E, Bryan MA, Chen W and Chen S, et al (2016). The transcription factor RUNX2 regulates receptor tyrosine kinase expression in melanoma. *Oncotarget* **7**, 29689–29707. https://doi.org/10.18632/oncotarget.8822.

[31] Prahallad A, Sun C, Huang S, Di Nicolantonio F, Salazar R and Zecchin D, et al (2013). Unresponsiveness of colon cancer to BRAF(V600E)inhibition through feedback activation of EGFR. *Nature* **482**, 100–103. https://doi.org/10.1038/nature10868.

[32] Mao M, Tian F, Mariadason JM, Tsao CC, Lemos R and Dayyani F, et al (2013). Resistance to BRAF inhibition in BRAF-mutant colon cancer can be overcome with PI3K inhibition or demethylating agents. *Clin Cancer Res* **19**, 657–667. https://doi.org/10.1158/1078-0432.CCR-11-1446.

[33] Corcoran RB, Atreya CE, Falchook GS, Kwak EL, Ryan DP and Bendell JC, et al (2015). Combined BRAF and MEK inhibition with dabrafenib and trametinib in BRAF V600-mutant colorectal cancer. *J Clin Oncol* **33**, 4023–4031. https://doi.org/10.1200/JCO.2015.63.2471.

[34] Kopetz S, Grothey A, Yaeger R, Van Cutsem E, Desai J and Yoshino T, et al (2019). Encorafenib, binimetinib, and cetuximab in BRAFV600E—mutated colorectal cancer. *N Engl J Med 2019. https://doi.org/10.1056/NEJMoa1908075. NEJMoa1908075—12.*

[35] Kim J-M, Yang Y-S, Park KH, Oh H, Greenblatt MB and Shim J-H (2019). The ERK MAPK pathway is essential for skeletal development and homeostasis. *Int J Mol Sci* **20**, 1803. https://doi.org/10.3390/ijms20081803.

[36] Banerji S, Cibulskis K, Rangel-Escareno C, Brown KK, Carter SL and Frederick AM, et al (2012). Sequence analysis of mutations and translocations across breast cancer subtypes. *Nature* **486**, 405—409. https://doi.org/10.1038/nature11154.

[37] Tentler JJ, Nallapareddy S, Tan AC, Spreafico A, Pitts TM and Morelli MP, et al (2010). Identification of predictive markers of response to the MEK1/2 inhibitor selumetinib (AZD6244) in K-ras-mutated colorectal cancer. *Mol Cancer Ther* **9**, 3351—3362. https://doi.org/10.1158/1535-7163.MCT-10-0376.

[38] Sun C, Hobor S, Bertotti A, Zecchin D, Huang S and Galimi F, et al (2014). Intrinsic resistance to MEK inhibitionin KRAS mutant lung and colon cancer through transcriptional induction of ERBB3. *Cell Rep* **7**, 86—93. https://doi.org/10.1016/j.celrep.2014.02.045.

[39] Ruess DA, Heynen GJ, Ciecielski KJ, Ai J, Berninger A and Kabacaoglu D, et al (2018). Mutant KRAS-driven cancers depend on PTPN11/SHP2 phosphatase. *Nat Med* **24**, 954—960. https://doi.org/10.1038/s41591-018-0024-8.

[40] Mainardi S, Mulero-Sánchez A, Prahallad A, Germano G, Bosma A and Krimpenfort P, et al (2018). SHP2 is required for growth of KRAS-mutant non-small-cell lung cancer in vivo. *Nat Med* **24**, 961—967. https://doi.org/10.1038/s41591-018-0023-9.

[41] Wong GS, Zhou J, Liu JB, Wu Z, Xu X and Li T, et al (2018). Targeting wild-type KRAS-amplified gastroesophageal cancer through combined MEK and SHP2 inhibition. *Nat Med* **24**, 968—977. https://doi.org/10.1038/s41591-018-0022-x.

[42] Shain AH, Garrido M, Botton T, Talevich E, Yeh I and Sanborn JZ, et al (2015). Exome sequencing of desmoplastic melanoma identifies recurrent NFKBIE promoter mutations and diverse activating mutations in the MAPK pathway. *Nat Genet* **47**, 1194—1199. https://doi.org/10.1038/ng.3382.

[43] Cohen-Solal KA, Boregowda RK and Lasfar A (2015). RUNX2 and the PI3K/AKT axis reciprocal activation as a driving force for tumor progression. *Mol Cancer 2015, 1—10. https://doi.org/10.1186/s12943-015-0404-3.*

[44] Tandon M, Chen Z and Pratap J (2014). Role of Runx2 in crosstalk between Mek/Erk and PI3K/Akt signaling in MCF-10A cells. *J Cell Biochem* **115**, 2208—2217. https://doi.org/10.1002/jcb.24939.